Design and global optimization of high-efficiency solar thermal systems with tungsten cermets

David Chester,[1] **Peter Bermel,**[1,2,3,4,*] **John D. Joannopoulos,**[1,2,3,4] **Marin Soljacic,**[1,2,3,4] **and Ivan Celanovic**[3]

[1]*Department of Physics, Massachusetts Institute of Technology, 77 Massachusetts Ave., Cambridge, Massachusetts 02139, USA*
[2]*Research Laboratory of Electronics, Massachusetts Institute of Technology, 77 Massachusetts Ave., Cambridge, Massachusetts 02139, USA*
[3]*Institute for Soldier Nanotechnologies, Massachusetts Institute of Technology, 77 Massachusetts Ave., Cambridge, Massachusetts 02139, USA*
[4]*Center for Materials Science and Engineering, Massachusetts Institute of Technology, 77 Massachusetts Ave., Cambridge, Massachusetts 02139, USA*
[*]*bermel@mit.edu*

Abstract: Solar thermal, thermoelectric, and thermophotovoltaic (TPV) systems have high maximum theoretical efficiencies; experimental systems fall short because of losses by selective solar absorbers and TPV selective emitters. To improve these critical components, we study a class of materials known as cermets. While our approach is completely general, the most promising cermet candidate combines nanoparticles of silica and tungsten. We find that 4-layer silica-tungsten cermet selective solar absorbers can achieve thermal transfer efficiencies of 84.3% at 400 K, and 75.59% at 1000 K, exceeding comparable literature values. Three layer silica-tungsten cermets can also be used as selective emitters for InGaAsSb-based thermophotovoltaic systems, with projected overall system energy conversion efficiencies of 10.66% at 1000 K using realistic design parameters. The marginal benefit of adding more than 4 cermet layers is small (less than 0.26%, relative).

OCIS codes: (230.5298) Photonic crystals; (350.6050) Solar energy.

References and links

1. W. Spirkl and H. Ries, "Solar thermophotovoltaics: an assessment," J. Appl. Phys. **57**, 4409–4414 (1985).
2. D. Y. Goswami, F. Kreith, and J. F. Kreider, *Principles of Solar Engineering* (Taylor and Francis, 2000).
3. F. J. DiSalvo, "Thermoelectric cooling and power generation," Science **285**, 703–706 (1999).
4. G. Chen, *Nanoscale Energy Transport and Conversion: a Parallel Treatment of Electrons, Molecules, Phonons, and Photons* (Oxford University Press, 2005).
5. H. H. Kolm, "Solar-battery power source," Quarterly Progress Report (1956), Group 35, p. 13.
6. B. Wedlock, "Thermo-photo-voltaic conversion," Proc. IEEE **51**, 694–698 (1963).
7. R. Black, P. Baldasaro, and G. Charache, "Thermophotovoltaics - development status and parametric considerations for power applications," in *International Conference on Thermoelectrics* (IEEE, 1999), Vol. 18, pp. 639–644.
8. F. O'Sullivan, I. Celanovic, N. Jovanovic, J. Kassakian, S. Akiyama, and K. Wada, "Optical characteristics of 1D Si/SiO2 photonic crystals for thermophotovoltaic applications," J. Appl. Phys. **97**, 033529 (2005).
9. N. Harder and P. Wurfel, "Theoretical limits of thermophotovoltaic solar energy conversion," Semicond. Sci. Technol. **18**, S151–S157 (2003).

#141815 - $15.00 USD Received 27 Jan 2011; revised 9 Mar 2011; accepted 10 Mar 2011; published 29 Mar 2011

10. P. Bermel, M. Ghebrebrhan, W. Chan, Y. X. Yeng, M. Araghchini, R. Hamam, C. H. Marton, K. F. Jensen, M. Soljacic, J. D. Joannopoulos, S. G. Johnson, and I. Celanovic, "Design and global optimization of high-efficiency thermophotovoltaic systems," Opt. Express **18**, A314–A334 (2010).
11. G. Rybicki and A. Lightman, *Radiative processes in astrophysics* (John Wiley and Sons, 1979).
12. C. Kennedy, "Review of mid- to high-temperature solar selective absorber materials," Tech. Rep. TP-520-31267, National Renewable Energy Laboratory (2002).
13. T. Sathiaraj, R. Thangarj, A. Sharbaty, M. Bhatnagar, and O. Agnihotri, "Ni-Al_2O_3 selective cermet coatings for photochemical conversion up to 500° C," Thin Solid Films **190**, 241 (1990).
14. Q.-C. Zhang, "High efficiency Al-N cermet solar coatings with double cermet layer film structures," J. Phys. D: Appl. Phys. **32**, 1938–1944 (1999).
15. P. Bienstman, "Rigorous and efficient modelling of wavelength scale photonic components," Ph.D. thesis, University of Ghent, Belgium (2001).
16. A. Rakic, A. Djurisic, J. Elazar, and M. Majewski, "Optical properties of metallic films for vertical-cavity optoelectronic devices," Appl. Opt. **37**, 5271–5283 (1998).
17. E. D. Palik, ed., *Handbook of Optical Constants of Solids* (Academic Press, 1998), Vol. 1.
18. R. Landauer, "Electrical conductivity in inhomogeneous media," (American Institute of Physics, 1978), Vol. 40, pp. 2–45.
19. P. Jepsen, B. Fischer, A. Thoman, H. Helm, J. Suh, R. Lopez, and R. Haglund, "Metal-insulator phase transition in a VO_2 thin film observed with terahertz spectroscopy," Phys. Rev. B **74**, 205103 (2004).
20. I. Celanovic, D. Perreault, and J. Kassakian, "Resonant-cavity enhanced thermal emission," Phys. Rev. B **72**, 075127 (2005).
21. S. Roberts, "Optical properties of nickel and tungsten and their interpretation according to Drude's formula," Phys. Rev. **114**, 104–115 (1959).
22. S. Kucherenko and Y. Sytsko, "Application of deterministic low-discrepancy sequences in global optimization," Comput. Optim. Appl. **30**, 297–318 (2005).
23. M. Powell, *Advances in Optimization and Numerical Analysis* (Kluwer Academic, 1994), pp. 51–67.
24. M. Ghebrebrhan, P. Bermel, Y. Avniel, J. D. Joannopoulos, and S. G. Johnson, "Global optimization of silicon photovoltaic cell front coatings," Opt. Express **17**, 7505–7518 (2009).

1. Introduction

Solar thermal, solar thermoelectrics, and solar thermophotovoltaics (TPV) offer three potentially high-efficiency paths for converting sunlight into electricity. All three ideally absorb sunlight strongly but have low thermal reradiation – a combination known as a selective solar absorber [1]. The heat can then be either used directly, or used to drive an electrical generator. In the most traditional case, heat is driven into a working fluid to run a mechanical engine [2]. Solar thermoelectrics instead use the Seebeck effect to generate electricity across a thermal gradient [3, 4]. In the case of solar TPV, as illustrated in Fig. 1, the selective absorber is thermally coupled to a selective emitter, which thermally radiates onto a nearby TPV cell capable of converting photons above the TPV bandgap energy directly into electricity [5–8]. The advantage of these approaches over traditional solar photovoltaics (PV) is that they can avoid two major sources of PV loss: thermalization of high-energy photons and reflection of low-energy photons. By absorbing almost all incoming solar photons as heat, and only re-radiating a small amount, the overall system efficiencies can approach the Carnot limit [9]. However, experimental systems have fallen well short of this ideal. A substantial amount of loss has been observed to occur both in selective solar absorbers as well as selective emitters, particularly under conditions of low concentration or high operating temperatures [10].

Ideal selective solar absorbers generally have strong solar absorption up to a cutoff wavelength, and very little beyond, in order to minimize thermal radiation predicted by Kirchoff's law [11]. There are multiple classes of structures designed specifically for selective absorption, such as intrinsic materials, semiconductor-metal tandems, multi-layer absorbers, metal-dielectric composite coatings, surface texturing, and coated blackbody-like absorbers [12]. Among these, metal-dielectric composites known as cermets are generally considered to have the greatest promise for high temperature applications (i.e., over 400 °C), with, for example, spectrally averaged absorbance of 0.94 and emittance of 0.07 for a single layer of graded Ni-

#141815 - $15.00 USD Received 27 Jan 2011; revised 9 Mar 2011; accepted 10 Mar 2011; published 29 Mar 2011

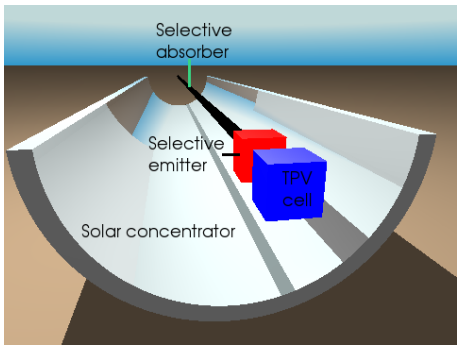

Fig. 1. Schematic illustration of a solar TPV system. Sunlight is collected via optical concentrators and sent to a selectively absorbing surface. That structure is thermally coupled to a selective emitter, which in conjunction with a filter, thermally emits photons with energies matched to the semiconductor bandgap of the TPV cell receiving them.

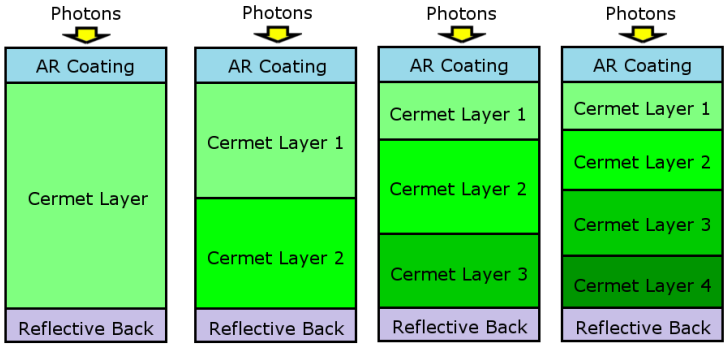

Fig. 2. Diagram depicting the layers of the cermet structures examined in this manuscript, which include a dielectric AR coating, back reflector, and 1-4 cermet layers in between.

Al_2O_3 cermet on stainless steel with an SiO_2 AR coating at 500 °C [13].

In this manuscript, we consider how to design the best possible cermet-based selective solar absorber. Our analysis begins by decomposing the basic structure into three components: an anti-reflection coating, a wavelength-sensitive absorber, and a highly reflective back. The anti-reflection coating increases the overall transmission of outside light into the absorber region. Ideally, the absorber itself will display strong absorption at short wavelengths, which rapidly diminishes beyond the cutoff. The reflective back ensures that unabsorbed light is rejected in the direction from whence it came. Previous research has shown that a stack of cermets can serve as an effective filter, because one can choose the metal volume fraction and thickness of each layer to obtain selective absorption [14]. Since in principle, metals and ceramics could be mixed with any metal volume fraction, thickness, and number of layers, it is clear that there is no simple way to determine what would be ideal, and that many possibilities have not yet been explored; hence, a numerical optimization approach is called for. This procedure is performed in this manuscript for the four separate but related structures depicted in Fig. 2.

We will present data which suggests that tungsten is a desirable metal for these applications because of its high melting point and suitable optical properties. Ideal optical properties result in reflection of low energy photons and absorption of high energy photons with a sharp cutoff

#141815 - $15.00 USD Received 27 Jan 2011; revised 9 Mar 2011; accepted 10 Mar 2011; published 29 Mar 2011

around the range needed for the semiconductor. Out of the many metals which were considered, tungsten is a strong candidate (if protected from reactions such as oxidation or silicide formation). Furthermore, tungsten has the highest melting point out of any pure metal, which is important for any high-temperature system. For these reasons, the following sections will demonstrate why tungsten cermets should offer the best performance for cermet-based selective absorbers and selective emitters.

The rest of this manuscript is structured as follows. The next section will explain the computational approach taken to accurately model the performance of cermets. It will then be followed by results and discussion, which will present the optimized results and compare it to previous research. In particular, it is shown that higher selective absorber efficiencies are theoretically possible with our optimized silica-tungsten cermets than any previously calculated selective absorber design.

2. Computational Approach

The University of Ghent developed the software package CAMFR, which can handle 1D and 2D structures [15]. With this software, the user can specify the refractive index of any material and stack multiple materials together. The thickness of each layer of the stack is also chosen by the user. CAMFR then calculates reflectance, transmittance, and absorptivity for the stack at each wavelength. Note that this calculation should be integrated over every angle, but normal incidence has been shown to be a good approximation in 1D structures for angles within $\pm\pi/3$ (which encompasses the vast majority of incoming and outgoing radiation). Next, the spectrally averaged absorptivity and emissivity can be calculated. The following thermal transfer efficiency is used as the figure of merit:

$$\eta_t = \frac{1}{CI}\int_0^\infty d\lambda\, \varepsilon(\lambda)\left[B\frac{dI}{d\lambda} - \frac{\pi hc^2}{\lambda^4\left(\exp(hc/\lambda kT)-1\right)}\right] \equiv B\alpha - \frac{\varepsilon\sigma T^4}{CI}, \tag{1}$$

where α and ε are the spectrally-averaged absorptivity and emissivity at a temperature T and solar concentration C, and B reflects absorption by the vacuum encapsulation system necessary to prevent convective heat losses (typically, $B = 0.91$ [14]).

Next, we can consider how to properly model the properties of cermets for arbitrary metal volume fractions between zero and one. First, a model for the constituent materials is required. The dielectrics can generally be modeled simply by constant refractive indices over the range of relevant wavelengths. Metals can be modeled by employing a Lorentz-Drude model matching the dispersion data provided in Refs. 16 and 17.

Modeling the interaction between the two requires employing solutions of Maxwell's equations based on differing assumptions about the interlocking microstructure of the ceramic and metallic regions. Two of the most well-known alternatives include the Bruggeman approximation [18] and the Maxwell-Garnett approximation [19] (also known as the Clausius-Mossotti relation [18]). They were both implemented numerically and compared to results from Refs. 13 and 14. While the Maxwell-Garnett approximation yields a close fit to experimental data at smaller metal fraction volumes, it fails for larger values above 0.4. By contrast, the Bruggeman approximation was found to be accurate over the entire range of physical metal volume fractions.

The Bruggeman approximation for the effective dielectric constant ε of two materials in three dimensions is given by:

$$v\frac{\varepsilon_m - \varepsilon}{\varepsilon_m + 2\varepsilon} + (1-v)\frac{\varepsilon_d - \varepsilon}{\varepsilon_d + 2\varepsilon} = 0, \tag{2}$$

where v and ε_m are the metal volume fraction and dielectric constant, respectively, and ε_d is

#141815 - $15.00 USD Received 27 Jan 2011; revised 9 Mar 2011; accepted 10 Mar 2011; published 29 Mar 2011

the ceramic dielectric constant. Fig. 3 plots the dielectric function for tungsten-silica cermets versus metal volume function as well as wavelength.

It was also an important goal to accurately model the optical properties of cermets over a wide range of temperatures. Ref. 20 offers a semi-empirical model for modifying the Lorentz-Drude equation to match experimental observations over a range of temperatures:

$$\Gamma_o(T) = \Gamma_o(T_o)\left(\frac{T}{T_o}\right)^{\alpha}. \tag{3}$$

The most obvious guess for α in a material with collisions dominated by phonons and a heat capacity following the law of Dulong and Petit is $\alpha = 1$. However, in order to obtain the best fit, we compared the predicted spectral emissivity for tungsten with measurements by Ref. 21 taken at the temperatures of 1100 K, 1600 K, 2000 K, and 2400 K. The best choice was found to be $\alpha = 0.85$. Fig. 4 graphs spectral emissivity versus wavelength for multiple temperatures. Our data matches Ref. 21 over a broad spectral range. Data points at two sample wavelengths, extracted from Ref. 21, are shown in Fig. 4.

Once the model was constructed, tested, and confirmed, the final step was to choose the right cermet structure. The next section will explain why tungsten was chosen as a metal. Once all of the materials were chosen, 1, 2, 3, and 4 layer cermets were constructed using CAMFR and then optimized using a global searching algorithm. The optimum was found using the multi-level single-linkage (MLSL), derivative-free algorithm with a low-discrepancy sequence (LDS) [22]. The efficiency equation shown above was chosen as the figure of merit to be optimized. All of the results were re-confirmed using other local algorithms, such as the NEWUOA algorithm of Powell [23]. All of these algorithms are contained in the NLopt package, freely available online at the URL `http://ab-initio.mit.edu/nlopt`. Fig. 5 displays a contour plot of the figure of merit of a two-layer cermet as a function of thicknesses for each cermet layer, with the other parameters set identical to the selective solar absorber at 400 K given in Table 3(b). It is evident that multiple local optima can by varying just two of the many optimization parameters for these systems, as has been shown in related systems [24].

3. Results and Discussion

The first step in designing an effective selective absorber was to choose the best metal for the cermet. Aluminum, nickel, tungsten, and chromium were considered. Aluminum and nickel were two metals that had been used in the previous works of Zhang and Sathiaraj, in that order [13, 14]. Tungsten and chromium were considered because of their high melting points and strong reflectivity in the infrared; however, tungsten displays stronger reflectivity above 2 μm where it is most needed, and has a much higher melting point than chromium, appropriate for high-temperature selective solar absorber applications. Next, the refractive index and spectral reflection of a Ni-Al_2O_3 cermet were compared to the data of Ref. 13 in order to confirm consistency. The same was done for a multilayer Al-AlON cermet which Ref. 14 had studied. Our Ni-Al_2O_3 model matches the experimental data of Ref. 13 accurately. Ref. 14 is a pure theory paper which uses a sputtered aluminum model that does not match ours perfectly, but nonetheless yields strong agreement in terms of emissivity spectra. These comparisons collectively confirm that our model is consistent with the literature on cermets.

In setting up our two material systems, silica (SiO_2) was chosen as the ceramic to be mixed with tungsten, primarily due to its low refractive index, while AlON was used in combination with aluminum, to facilitate direct comparison with the results of Ref. 14. Ref. 14 only used 2 and 9 cermet layers in his structures and then suggested that using 9 layers does not offer a significant efficiency advantage compared to 2. However, it is possible that the extremely large

#141815 - $15.00 USD Received 27 Jan 2011; revised 9 Mar 2011; accepted 10 Mar 2011; published 29 Mar 2011

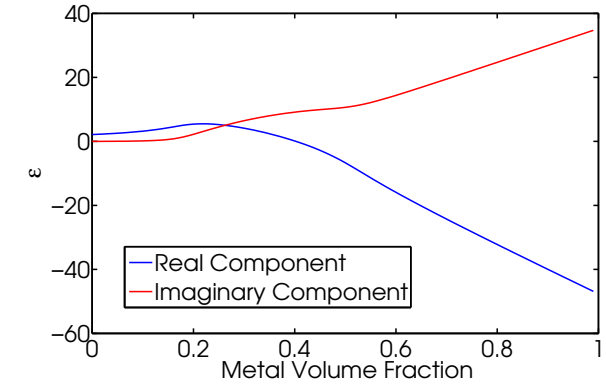

(a)

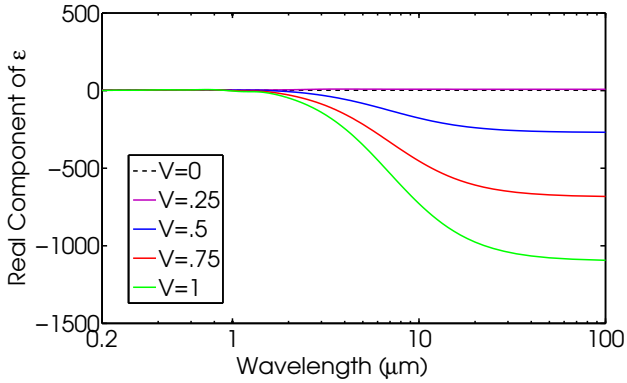

(b)

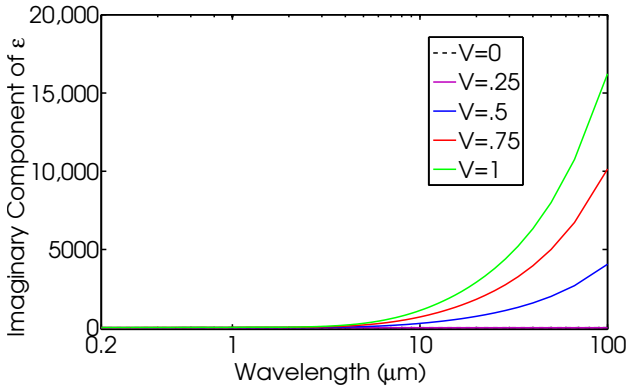

(c)

Fig. 3. Behavior of the dielectric constants associated with the Bruggeman approximation (a) as a function of metal volume fraction ($\lambda = 2\,\mu$m) (b) as a function of wavelength (real part) and (c) as a function of wavelength (imaginary part).

#141815 - $15.00 USD Received 27 Jan 2011; revised 9 Mar 2011; accepted 10 Mar 2011; published 29 Mar 2011

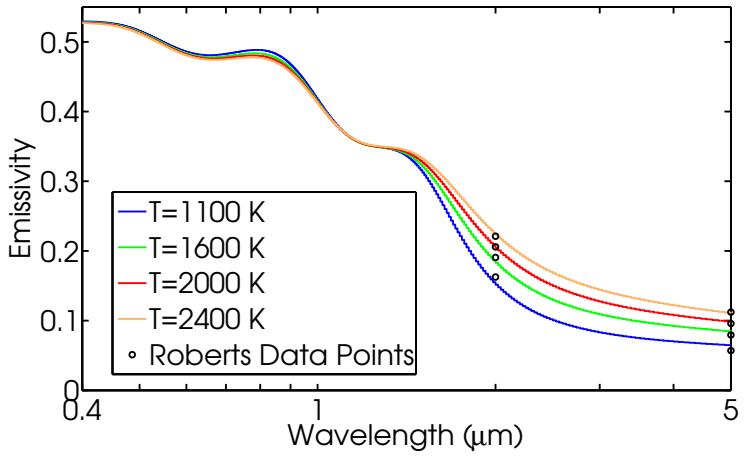

Fig. 4. Emissivity spectrum of tungsten for various temperatures both in experiment (circles) and in our numerical model (lines).

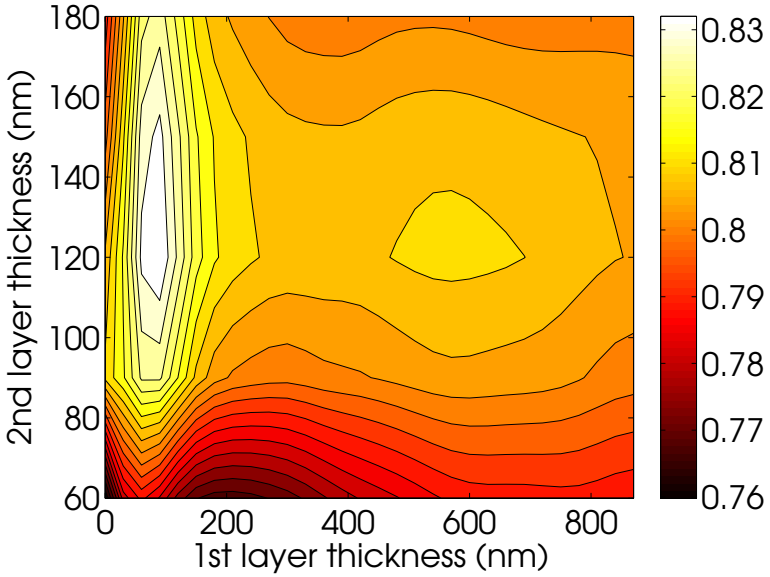

Fig. 5. The figure of merit for a two-layer cermet selective absorber as a function of cermet thicknesses for the first and second layers. The rest of the parameters are from the optimized two layer structure, with the other parameters set identical to the selective solar absorber at 400 K given in Table 3(b).

#141815 - $15.00 USD Received 27 Jan 2011; revised 9 Mar 2011; accepted 10 Mar 2011; published 29 Mar 2011

phase space of the 9-layer system was not fully explored, since his 9-layer design is almost identical to the 2-layer one. One of our goals is to use a global optimization on 1 through 4 cermet layers to determine if there was any advantage to adding more than 2 layers.

With the selective solar absorber structures thus chosen, we then proceed to employ the techniques outlined in Section 2 to calculate and then optimize our aluminum and tungsten designs. This optimization is performed for two different operating conditions, roughly in line with known solar applications. Our first condition is an operating temperature of 400 K with no solar concentration; our second condition is an operating temperature of 1000 K with a concentration of 100 suns. Since Refs. 13 and 14 quote their spectrally averaged absorptivity and emissivity, these numbers can be used in the same thermal efficiency equation for a direct comparison. Refs. 13 and 14 perform their analysis at 353 K and 373 K, respectively. It is known that as the temperature increases, thermal efficiency decreases, so the efficiencies they calculated are lower at our target temperatures of 400 K and 1000 K. Also, some more recent work has directly considered efficiencies for multiple structures at 400 K and 1000 K [10]. Only the full set of tungsten-silica cermet designs were fully optimized at 400 K and 1000 K, after it became apparent that it would perform better than the aluminum structure. Table 1 shows the efficiencies at 400 K and 1000 K for 1-4 layer cermet structures with AR coatings (illustrated in Fig. 2), as well as the calculated equivalent efficiency for other structures. Figures 6 and 7 show the reflection spectrum as well as metal volume fraction versus thickness for 1-4 layer cermets at 400 K and 1000 K, respectively.

Table 1. Spectrally Averaged Absorptivities α, Emissivities ε, and Thermal Transfer Efficiencies η_t for 1-4 Layer Tungsten–Silica Cermet Structures (Illustrated in Fig. 2) Compared to Other Selective Absorbers at 400 K with Unconcentrated Sunlight, and 1000 K with Concentration of 100 Suns

Selective Absorber Structure	$\alpha(400)$	$\varepsilon(400)$	$\eta_t(400)$	$\alpha(1000)$	$\varepsilon(1000)$	$\eta_t(1000)$
Optimized 1 Layer Cermet	0.945	0.033	0.822	0.908	0.161	0.7282
Optimized 2 Layer Cermet	0.967	0.038	0.836	0.945	0.172	0.7556
Optimized 3 Layer Cermet	0.977	0.042	0.840	0.946	0.173	0.7558
Optimized 4 Layer Cermet	0.979	0.042	0.843	0.945	0.172	0.7559
SiO_2 + Ni-Al_2O_3 cermet [13]	0.94	0.07	0.776	-	-	-
3 layer AlON cermet + Al_2O_3 AR [14]	0.974	0.055	0.824	-	-	-
4 FCs + Ge + 1 BC + Ag [10]	0.907	0.016	0.807	-	-	-
1 FC + Si + Ag [10]	-	-	-	0.766	0.089	0.596
4 FCs + Si + 1 BC + Ag [10]	-	-	-	0.868	0.073	0.707

Our tungsten cermet selective absorbers offer unmatched efficiency plus robustness to small parameter changes. Not only are they more efficient than Refs. 13 and 14, despite operating at a slightly higher temperature of 400 K, but they appear to offer strong performance at the less well-explored regime of temperatures close to 1000 K [12] as well. At 400 K, our 4 layer cermet structure has a thermal efficiency at 84.3%, while the best structure found in the literature has an equivalent efficiency of 82.4%. Our optimized 4-layer cermet has an efficiency of 75.59%, while the previous best value in the literature was 70.7% [10]. A graphical representation of the thickness and metal volume fraction of each layer is given in Fig. 6 for designs optimized at 400 K for unconcentrated sunlight, and in Fig. 7 for designs optimized at 1000 K for 100 suns. Table 3. Note that these results are robust with respect to small variations of input parameters such as layer thicknesses, refractive indices, and metal volume fractions. In particular, the thermal transfer efficiencies remain within 1% of their maximum value for variations of $\pm$15% of the layer thickness and refractive index. Adding surface roughness would be

#141815 - $15.00 USD Received 27 Jan 2011; revised 9 Mar 2011; accepted 10 Mar 2011; published 29 Mar 2011

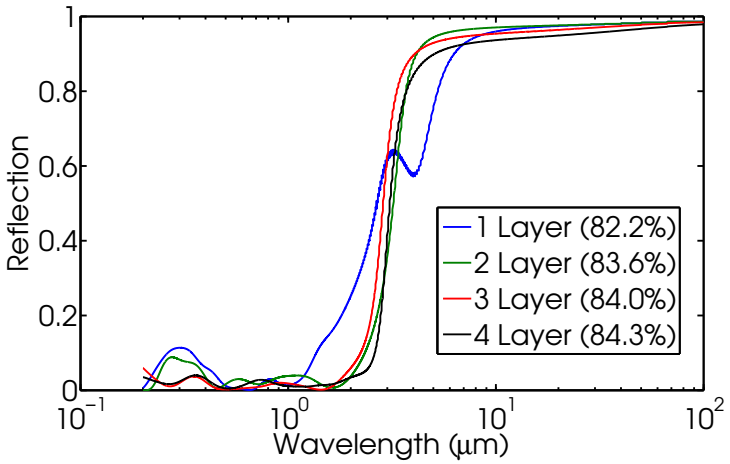

(a)

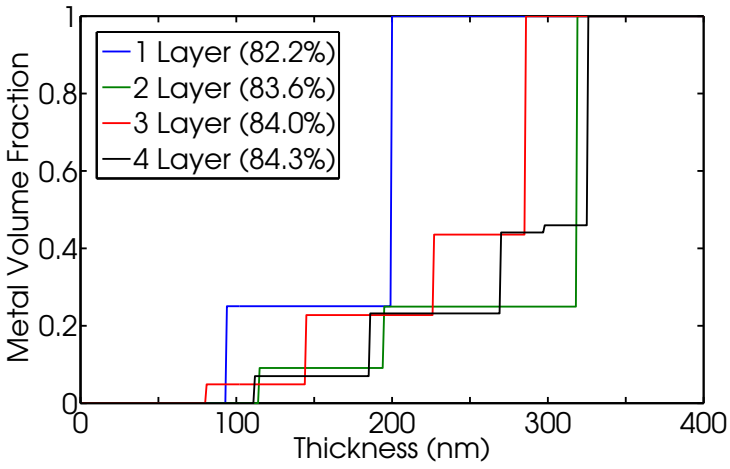

(b)

Fig. 6. For silica-tungsten cermet selective absorbers with C=1 at 400 K: (a) Optimized reflection spectra for 1-4 layer structures (b) corresponding metal volume fractions as a function of thickness for optimized structures of 1-4 layers.

#141815 - $15.00 USD Received 27 Jan 2011; revised 9 Mar 2011; accepted 10 Mar 2011; published 29 Mar 2011

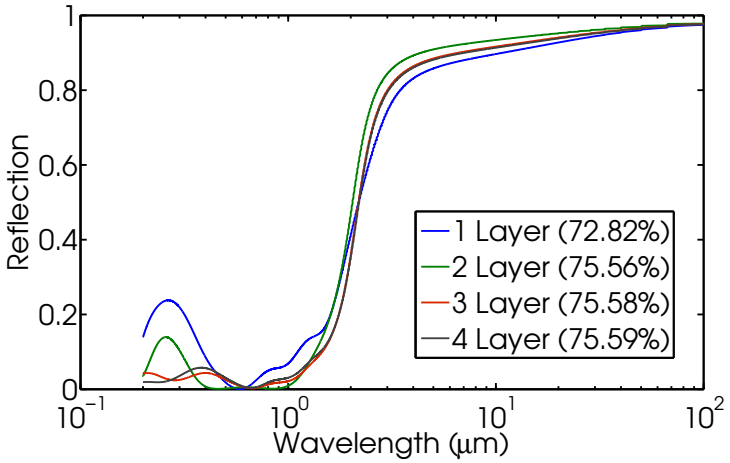

(a)

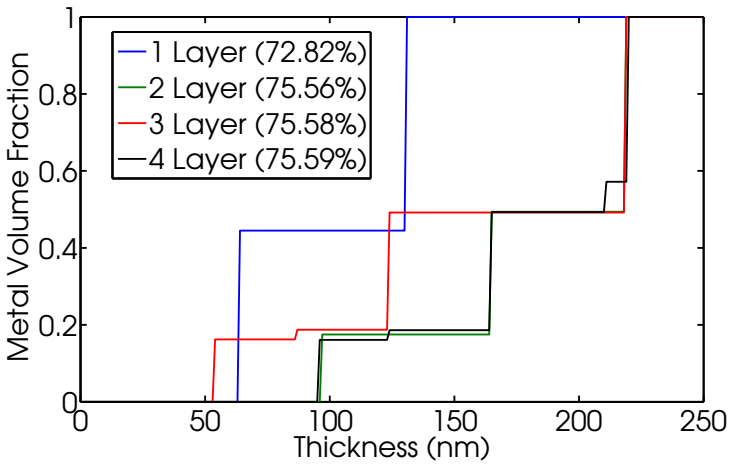

(b)

Fig. 7. For silica-tungsten cermet selective absorbers with C=100 at 1000 K: (a) Optimized reflection spectra for 1-4 layer structures (b) corresponding metal volume fractions as a function of thickness for optimized structures of 1-4 layers.

#141815 - $15.00 USD Received 27 Jan 2011; revised 9 Mar 2011; accepted 10 Mar 2011; published 29 Mar 2011

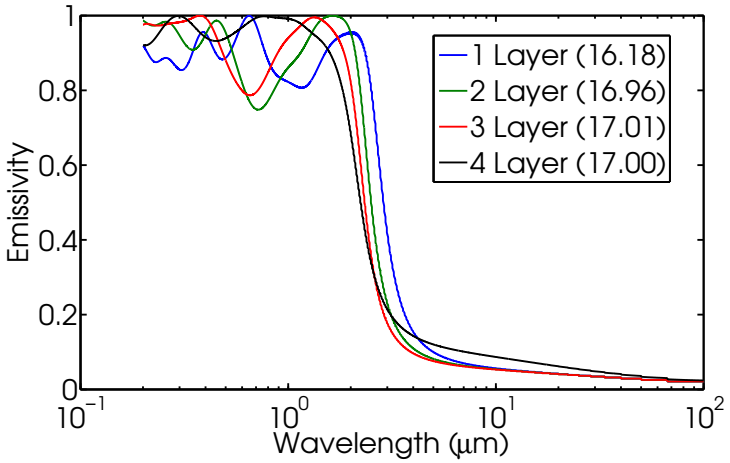

(a)

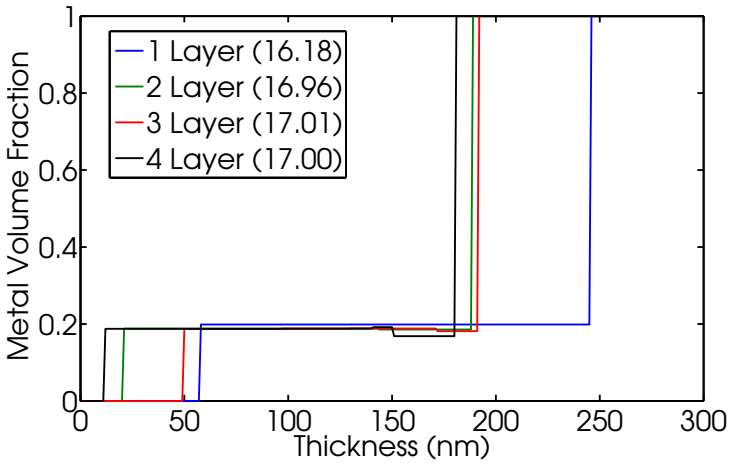

(b)

Fig. 8. For silica-tungsten cermet selective emitters at 1000 K: (a) Optimized emissivity spectra for 1-4 layer structures (b) Metal volume fraction as a function of thickness for optimized 1-4 layer structures.

expected to uniformly decrease overall performance along the lines of Mie theory, with weak scattering and negligible impact on performance for small features, but rising rapidly as feature size approaches half the target wavelength.

Tungsten-silica cermets were also optimized for selective emitter applications using the same global optimization techniques of the selective absorbers. The figure of merit chosen for these structures was the product of efficiency and power for a system comprised of an emitter at 1000 K with a surface area of 1 cm^2 on both sides, matched at negligible separation from two TPV diodes of equal area, made from InGaAsSb (with a bandgap of 0.547 eV), with an external quantum efficiency of 82%, shadowing of 10%, device temperature of 300 K, ideality factor of 1.171, and a dark current of 18 $\mu A/cm^2$. Other parameters were as in Section 3 of Ref. [10]. Table 2 shows the figures of merit achieved for 1-4 layer tungsten-silica cermets, while Table 3

#141815 - $15.00 USD Received 27 Jan 2011; revised 9 Mar 2011; accepted 10 Mar 2011; published 29 Mar 2011

Table 2. Overall Figures of Merit (Defined as Efficiency Times Power Output of System Based on Ref. [10]) for 1-4 Layer Tungsten–Silica Cermet Selective Emitter Structures

Selective Emitter Structure	FOM
Optimized 1 Layer Cermet	16.18
Optimized 2 Layer Cermet	16.96
Optimized 3 Layer Cermet	17.01
Optimized 4 Layer Cermet	17.00

provides the optimized parameters producing the figures of merit in its last column. Figure 8(a) graphs the emissivity spectrum for optimized structures consisting of AR coatings plus 1-4 layer cermets (illustrated in Fig. 2); Fig. 8(b) shows the metal volume fraction as a function of position for optimized cermet structures. The best FOM for selective emitters found was 17.01, which is substantially better than previous FOMs found for 1D photonic crystal structures of 9.79, and platinum structures coated with silica of 10.35 [10]. This corresponds to a projected experimental efficiency of 10.66%, greater than the efficiency of many thermoelectric systems [3]. Thus, tungsten-silica cermets appear to be a good choice for selective emitters as well as selective absorbers.

4. Conclusions

In this paper, we examined the basic physical mechanism for the operation of selective absorbers and emitters based on cermets. We explored a wide range of metals and dielectric materials that could be employed in fabricating a high-performance design, and suggested a combination of tungsten and silica is optimal. It was found that subdividing the cermet layer into multiple layers with varying metal volume fractions and globally optimizing using the software package NLopt yields gradually increasing performance, although there appears to be a law of diminishing returns when adding more layers. To the best of our knowledge, the overall performance of the optimized 4-layer selective solar absorber exceeds anything else found in the literature, even compared to a 9-layer design in Ref. [14], with a thermal transfer efficiency of 84.3% for 400 K and unconcentrated sunlight, and an efficiency of 75.59% for 1000 K at 100 suns concentration. Furthermore, it was found that a separately optimized but similar 3-layer selective emitter design could yield an energy conversion efficiency of 10.66% for a TPV system as a whole, exceeding other 1D designs of equal or greater complexity. In future work, the role of angular dependence will be explored, and additional optical elements will be introduced to yield higher and even more realistic performance predictions.

Acknowledgments

We thank Yi Xiang Yeng for valuable discussions. This work was supported in part by the MRSEC Program of the National Science Foundation under award number DMR-0819762, the MIT S3TEC Energy Research Frontier Center of the Department of Energy under Grant No. DE-SC0001299, and the Army Research Office through the Institute for Soldier Nanotechnologies under Contract Nos. DAAD-19-02-D0002 and W911NF-07-D0004.

#141815 - $15.00 USD Received 27 Jan 2011; revised 9 Mar 2011; accepted 10 Mar 2011; published 29 Mar 2011

Table 3. Parameters for 1-4 Layer Tungsten–Silica Cermet Structures at 400 K and 1000 K for (a) 1-Layer Cermets, (b) 2-Layer Cermets, (c) 3-Layer Cermets, and (d) 4-Layer Cermets (All Thicknesses in nm)

(a)

1 Layer Parameters	Sel. Absorber (400 K)	Sel. Absorber (1000 K)	Sel. Emitter (1000 K)
AR refractive index	1.44	1.78	1.79
AR thickness	91.1	62.6	57.1
Cermet volume fraction	.2506	.4438	.1988
Cermet thickness	107.7	67.1	188.9

(b)

2 Layer Parameters	Sel. Absorber (400 K)	Sel. Absorber (1000 K)	Sel. Emitter (1000 K)
AR refractive index	1.24	1.24	1.46
AR thickness	114.3	96.3	20.0
Cermet 1 volume fraction	.0910	.1751	.1882
Cermet 1 thickness	80.1	68.3	123.5
Cermet 2 volume fraction	.2495	.4939	.1858
Cermet 2 thickness	124.5	54.4	45.2

(c)

3 Layer Parameters	Sel. Absorber (400 K)	Sel. Absorber (1000 K)	Sel. Emitter (1000 K)
AR refractive index	1.25	1.24	1.25
AR thickness	79.8	53.8	49.3
Cermet 1 volume fraction	.0487	.1622	.1874
Cermet 1 thickness	64.5	33.6	80.5
Cermet 2 volume fraction	.2277	.1874	.1885
Cermet 2 thickness	82.0	37.3	42.0
Cermet 3 volume fraction	.4356	.4918	.1816
Cermet 3 thickness	58.9	95.7	20.0

(d)

4 Layer Parameters	Sel. Absorber (400 K)	Sel. Absorber (1000 K)	Sel. Emitter (1000 K)
AR refractive index	1.24	1.24	1.50
AR thickness	109.6	95.0	11.0
Cermet 1 volume fraction	.0651	.1607	.1877
Cermet 1 thickness	74.3	27.4	85.4
Cermet 2 volume fraction	.2324	.1849	.1882
Cermet 2 thickness	83.9	41.6	42.9
Cermet 3 volume fraction	.4265	.4926	.1918
Cermet 3 thickness	27.8	45.7	10.0
Cermet 4 volume fraction	.4596	.5717	.1684
Cermet 4 thickness	28.5	9.5	30.2

#141815 - $15.00 USD Received 27 Jan 2011; revised 9 Mar 2011; accepted 10 Mar 2011; published 29 Mar 2011